



# Microevolution of the *mexT* and *lasR* Reinforces the Bias of Quorum Sensing System in Laboratory Strains of *Pseudomonas aeruginosa* PAO1

Yang Liu<sup>1,2†</sup>, Stephen Dela Ahator<sup>1,3†</sup>, Huishan Wang<sup>1</sup>, Qishun Feng<sup>1</sup>, Yinuo Xu<sup>1</sup>, Chuhao Li<sup>1</sup>, Xiaofan Zhou<sup>1\*</sup> and Lian-Hui Zhang<sup>1\*</sup>

## OPEN ACCESS

### Edited by:

Liang Wang,  
Xuzhou Medical University, China

### Reviewed by:

Margarita Gomila,  
University of the Balearic Islands,  
Spain

Yongjun Tang,  
Shenzhen Polytechnic, China

### \*Correspondence:

Xiaofan Zhou  
xiaofan\_zhou@scau.edu.cn  
Lian-Hui Zhang  
lhzhang01@scau.edu.cn

<sup>†</sup>These authors have contributed  
equally to this work and share first  
authorship

### Specialty section:

This article was submitted to  
Evolutionary and Genomic  
Microbiology,  
a section of the journal  
*Frontiers in Microbiology*

Received: 24 November 2021

Accepted: 16 February 2022

Published: 12 April 2022

### Citation:

Liu Y, Ahator SD, Wang H, Feng Q, Xu Y, Li C, Zhou X and Zhang L-H (2022) Microevolution of the *mexT* and *lasR* Reinforces the Bias of Quorum Sensing System in Laboratory Strains of *Pseudomonas aeruginosa* PAO1. *Front. Microbiol.* 13:821895. doi: 10.3389/fmicb.2022.821895

<sup>1</sup> Guangdong Province Key Laboratory of Microbial Signals and Disease Control, Integrative Microbiology Research Centre, South China Agricultural University, Guangzhou, China, <sup>2</sup> Centro de Biotecnología y Genómica de Plantas, Universidad Politécnica de Madrid (UPM) – Instituto Nacional de Investigación y Tecnología Agraria y Alimentaria (INIA), Madrid, Spain, <sup>3</sup> Research group for Host Microbe Interactions, Department of Medical Biology, Faculty of Health Sciences, UiT The Arctic University of Norway, Tromsø, Norway

The *Pseudomonas aeruginosa* strain PAO1 has routinely been used as a laboratory model for quorum sensing (QS). However, the microevolution of *P. aeruginosa* laboratory strains resulting in genetic and phenotypic variations have caused inconsistencies in QS research. To investigate the underlying causes of these variations, we analyzed 5 *Pseudomonas aeruginosa* PAO1 sublines from our laboratory using a combination of phenotypic characterization, high throughput genome sequencing, and bioinformatic analysis. The major phenotypic variations among the sublines spanned across the levels of QS signals and virulence factors such as pyocyanin and elastase. Furthermore, the sublines exhibited distinct variations in motility and biofilm formation. Most of the phenotypic variations were mapped to mutations in the *lasR* and *mexT*, which are key components of the QS circuit. By introducing these mutations in the subline PAO1-E, which is devoid of such mutations, we confirmed their influence on QS, virulence, motility, and biofilm formation. The findings further highlight a possible divergent regulatory mechanism between the LasR and MexT in the *P. aeruginosa*. The results of our study reveal the effects of microevolution on the reproducibility of most research data from QS studies and further highlight *mexT* as a key component of the QS circuit of *P. aeruginosa*.

**Keywords:** *Pseudomonas aeruginosa* PAO1, *mexT*, *lasR*, quorum sensing, microevolution, *mexT* evolution, *mexT* selection pressure, *mexT* Indel

## INTRODUCTION

*Pseudomonas aeruginosa* causes acute and chronic infections in immune-compromised individuals and cystic fibrosis (CF) sufferers (Stover et al., 2000). Infections by *P. aeruginosa* are usually difficult to treat and persistent due to the characteristic high frequency of emergence of antimicrobial-resistant strains during therapy and the ability to switch to a biofilm state under

stress conditions (Carmeli et al., 1999). As a metabolically versatile bacterium, it can adapt to myriads of environments by sensing and altering its genetic regulations to cope with imminent stress conditions. These traits have been shown to be dependent on quorum sensing (QS), the cell-density dependent regulatory mechanisms that coordinate genetic regulation in response to chemical signals or cues present in its environment (Jensen et al., 2006).

*Pseudomonas aeruginosa* QS is composed of three main signals, N-(3-oxododecanoyl)-L-homoserine lactone (3-oxo-C12-HSL, 3OC12HSL), N-butanoyl-L-homoserine lactone (C4-HSL, C4HSL), and 2-heptyl-3-hydroxy4(1H)-quinolone (PQS), which are produced by the *lasI*, *rhlI*, and *pqsABCDH* gene cluster, respectively. These signals bind to their cognate regulators LasR, RhlR, and PqsR(MvfR) to activate downstream virulence factors such as pyocyanin, elastase, rhamnolipids, and pyoverdine (Schuster and Greenberg, 2006; Eickhoff and Bassler, 2018). In addition, an integrative QS signal (IQS) has also been identified, which could take over the role of upstream *las* system to regulate the downstream QS systems including *rhl* and *pqs* (Lee et al., 2013). The production of signals and expression of receptors can be regulated at the transcriptional level by a series of regulators and other metabolic systems. These include the negative regulators MvaT, QscR, QslA, QteE, RpoN, RpoS, and RsaL, and positive regulators GacA/GacS, Vfr, and VqsR (Lee and Zhang, 2015). The elaborate network of regulatory pathways which make up the QS circuit in *P. aeruginosa* creates a signaling continuum allowing for an effective response to varying cues which is vital for fine-tuning the adaptation of the bacterium to imminent stress conditions (Ahator and Zhang, 2019).

The adaptive processes required for the survival of *P. aeruginosa* isolates are driven by selective mutations resulting in genetic and phenotypic variations, in response to the selection pressures encountered during infection in the host and external environment (Cordero and Polz, 2014; Lee and Zhang, 2015; Hussain et al., 2022). Spontaneous mutations in the QS regulators *lasR*, *rhlR*, and their cognate synthases *lasI* and *rhlI*, are frequently identified in *P. aeruginosa* clinical isolates (Hoffman et al., 2009). These mutations result in attenuation of virulence observed in the switch from acute to chronic infection states, biofilm to planktonic lifestyle transition, and increased fitness and growth advantage in polymicrobial settings (Köhler et al., 2009; Wilder et al., 2011). Additionally, mutations occurring in the *gacS*, *retS*, *ampR*, and the multidrug efflux pump regulators drive the switch from acute to chronic infectious states and antimicrobial resistance (Balasubramanian et al., 2014; Winstanley et al., 2016). Similarly, mutations in the multi-drug resistance regulatory gene *mexT* which regulates the MexEF-OprN system and negatively regulates OprD have been shown to drive resistance to antibiotics in clinical isolates (Horna et al., 2018; Juarez et al., 2018). Also, *mexT* has been shown as a major factor in the regulation of QS-associated factors and fitness of *P. aeruginosa*. This role is due to its global regulon which intersect the *las-pqs-rhl* hierarchical QS circuit (Kostylev et al., 2019).

Recent studies have also identified genetic and phenotypic diversification among the laboratory strain PAO1 from different

laboratories (Klockgether et al., 2010; Chandler et al., 2019). The studies revealed sublines of PAO1 exhibiting variability in metabolism, virulence, and cell-cell signaling (Preston et al., 1995; Davies and Davies, 2010; Klockgether et al., 2010) which were proposed to arise due to prolonged propagation in selective growth media (Klockgether et al., 2010). The genetic and phenotypic diversification in the sublines have been of broad interest, due to the evidence and impact of microevolution in the sublines presented in these studies. As PAO1 is commonly used for QS research, such variations could have a significant impact on the reproducibility of research data. Although these studies showed the phylogenetic relationship between various sublines based on their genome composition and mutations, the genetic mechanisms that influence the phenotypic variations among the sublines and their impact on the variations in QS remain vague.

Our lab uses the *P. aeruginosa* PAO1 as a model organism for investigating the regulation of the population density dependent cell-cell communication mechanism (QS) and its associated virulence factors and stress response. An in-house experimental analysis of QS phenotypes from our lab collections of *P. aeruginosa* PAO1 revealed differences in QS-related factors among the sublines. This prompted an investigation for the underlying factors driving such variations in phenotypes. To identify the underlying causes for such phenotypic variations among the PAO1 sublines, we analyzed the genetic and phenotypic diversity of 4 *P. aeruginosa* PAO1 sublines obtained from our laboratory (Lian-Hui Zhang) collection and a subline from E. Peter Greenberg Lab (University of Washington) in terms of their variations in the production of QS-related factors, biofilm, and motility. We also combined high throughput genome sequencing, bioinformatic analysis, and genomic manipulation of the sublines to identify key mutations driving such variations. We were able to map the mutations in the *lasR* and *mexT* as driving factors of the microevolution of the lab strains and explain their potential effect on cell-to-cell signaling and virulence in *P. aeruginosa*.

## MATERIALS AND METHODS

### Bacterial Strains and Growth Conditions

The *P. aeruginosa* PAO1 strains used in this study are listed in Table 1. All strains were maintained in 40% glycerol, 60% Lysogeny Broth (LB, 1 /L, 15 g Agar, 10 g Tryptone [Sigma-Aldrich], 5 g Yeast Extract [Sigma-Aldrich], 10 g NaCl) at  $-80^{\circ}\text{C}$ . For all experiments, cultures were inoculated directly from the stock used for sequencing without subculturing.

### Genomic DNA Extraction and Whole Genomic Sequences

The EasyPure Bacteria Genomic DNA Kit (EE161-01, Transgenbiotech, Beijing, China) was used for the extraction of the genomic DNA from the sublines. The concentration of genomic DNA was measured by NanoDrop and stored at  $-20^{\circ}\text{C}$ . The genomic DNA of the five sublines was sequenced using the Illumina NovaSeq S4 PE-150 (Novogene, China) and Oxford Nanopore MinION (Nextomics Biosciences, China).

**TABLE 1 |** Strain selection and genome characteristics.

Strain name	Source	NCBI BioSample accession no.	Genome size (bp)	GC content(%)
PAO1-A	Integrative Microbiology Research Centre, SCAU (China)	SAMN13612472	6,288,998	66.48
PAO1-B	Integrative Microbiology Research Centre, SCAU (China)	SAMN13612473	6,226,774	66.55
PAO1-C	Integrative Microbiology Research Centre, SCAU (China)	SAMN13612474	6,266,737	66.53
PAO1-D	Integrative Microbiology Research Centre, SCAU (China)	SAMN13612475	6,220,344	66.58
PAO1-E	University of Washington (United States)	SAMN13612476	6,275,136	66.54

All PAO1 subline NCBI accession numbers are listed.

## Genome Assembly, Mapping, and Genome Annotation

Sequences were checked by FastQC software (Andrews, 2010), a quality control tool for high throughput raw data. Short reads (coverage 300×) were mapped against the reference using Burrows-Wheeler Aligner BWA-MEM (Li and Durbin, 2009). *De novo* assembly by both short reads and long reads was performed using Unicycler (Wick et al., 2017) with SPAdes algorithm and hybrid assembled data summarized by BBMap (Bushnell, 2014). The DFAST (Tanizawa et al., 2018) was used for gene prediction and annotation.

## SNP Detection and Analysis

A combination of software was used for SNPs calling. The SAMtools, bcftools (Li, 2011) and GATK Best Practices (Depristo et al., 2011; Van der Auwera et al., 2013) were used for variant calling workflow. The bcftools calling were trimmed by removing MIN(QUAL) < 100 SNPs. GATK SNPs calling were followed by germline short variant discovery (SNPs + Indels) using HaplotypeCaller and GenotypeGVCFs tools (Poplin et al., 2017). SNPs were further trimmed by removing MIN(QUAL) < 500. SNPs were also identified in the assembled data generated by the Unicycler using Mummer (Kurtz et al., 2004) and progressive Mauve (Darling et al., 2010). The SNPs produced by the four tools were merged and false-positive SNPs eliminated by checking the original mapped short reads bam file manually using IGV (Robinson et al., 2011). The supporting reads which were less than 25% were not considered as SNPs.

## Structure Variation Detection and Analysis

Integrated structural variant multiple callers were used to detect SVs. The Structural Variants from Mummer svmu (Chakraborty et al., 2018) tool was used to compare *de novo* assembly sequence against the reference. BreakDancer (Chen et al., 2009) was used to set sorted mapping input bam files and filter the total number of reads pairs > 3 or confidence score > 85%. Using Pindel (Ye et al., 2009), which operates on a read-pair based method, the outputs allele depth (AD) over 20% were kept and for split-reads based DELLY (Rausch et al., 2012), and the outputs paired-end supported site (PE) < 2 were discarded. Also, Svseq2 (Zhang et al., 2012) was used to detect deletions and insertions. All results were merged to obtain a final list of SVs by a union of the output from the individual callers. A diagrammatic representation of the filter parameter is shown in **Supplementary Figure 1**.

## SNPs and Structure Variation Annotation

The common SNPs and SVs in the sublines were manipulated by the command line script to separate from individual variation. All SNPs and SVs were customized into a VCF file on demand by the shell script. SnpEff (Cingolani et al., 2012) was used for variation annotation to predict the effect of the genetic variants against the *Pseudomonas aeruginosa* PAO1 SnpEff database.

## Selective Pressure of *Pseudomonas aeruginosa* Single-Copy Genes

The raw data (Pseudomonas Ortholog Groups) used for the mutation rate analysis was collected from Pseudomonas Genome Database (Winsor et al., 2016) (v18.1). The downloaded Ortholog files were filtered by the python script (see **Supplementary Material**) to obtain only 4,419 single-copy gene and 298 *Pseudomonas aeruginosa* strains (see **Supplementary Material**). The nucleotide sequences were extracted by the mapping gene ID with the strain name to Pseudomonas Genome Database (v18.1) Annotations (GFF3) and Genomic DNA (FASTA) files. Single-copy gene files were translated by the EMBOSS Transeq tool (Rice et al., 2000), aligned by the mafft tool (parameter:retree 1) (Katoh, 2002). The codon alignment was generated through the pal2nal.pl (Suyama et al., 2006) program and the alignment files were trimmed by trimAl (parameter:gappyout) (Capella-Gutierrez et al., 2009). The required treefile for subsequent analysis was generated by iqtree (parameter:st = DNA m = GTR+G4 nt = 1 fast) (Nguyen et al., 2015) for single-copy gene files, individually. The mutation rate of each single-copy gene was calculated by HyPhy-Branch-Site Unrestricted Statistical Test for Episodic Diversification (hyphy BUSTED) (Murrell et al., 2015). Nonsynonymous/synonymous (dN/dS) ratio were generated by improving branch lengths, nucleotide substitution biases, and global dN/dS ratios under a full codon model. The mutation rates are in **Supplementary Table 3**.

## Estimate Mean Posterior Synonymous Substitution Rate and Mutational Type of *Pseudomonas aeruginosa lasR* and *mexT* Gene Site

The *lasR* and *mexT* sequences were blasted against all *P. aeruginosa* complete and draft genome in the Pseudomonas Genome Database (v18.1). Codon alignment of the *lasR* (2498) and *mexT* (2643) sequences was performed by transeq, mafft, and pal2nal tools. The multiple sequence alignments files were trimmed by the python script to make them inframe and remove

the stop codon. The mutation rate of each site was calculated by hyphy FUBAR (Murrell et al., 2013). The mutational types were calculated via Biopython (Peter et al., 2009).

## In-Frame Deletion and Knock-In

DNA manipulation was conducted by In-frame deletions and insertion described previously (Filloux and Ramos, 2014). The DNA fragments for 3 bp insertion in *lasR* and 18 bp deletion in *mexT* mutations were synthesized by Sangon Biotech (China). The fragments were cloned into pK18mobsacB plasmid using ClonExpress MultiS One Step Cloning Kit (C113-01, Vazyme) for construction gene knock-in and deletion constructs. The constructs were transformed into *E. coli* S17-1 for conjugation with PAO1-E. Transconjugants were selected on Minimal Media (MM; per liter containing mannitol, 2.0 g;  $(\text{NH}_4)_2\text{SO}_4$ , 2.0 g;  $\text{K}_2\text{HPO}_4$ , 10.5 g;  $\text{KH}_2\text{PO}_4$ , 4.5 g;  $\text{MgSO}_4 \cdot 7\text{H}_2\text{O}$ , 2.0 g;  $\text{FeSO}_4$ , 5 mg;  $\text{CaCl}_2$ , 10 mg;  $\text{MnCl}_2$ , 2 mg; pH 7.0) supplemented with gentamicin (30  $\mu\text{g}/\text{mL}$ ) and transferred onto MM supplemented with 10% (wt/vol) sucrose to select mutants. Mutants containing the desired deletion and insertion were confirmed by PCR and DNA Sanger sequencing.

## Motility

Motility was assayed by the Plate-Based method as previously described (Filloux and Ramos, 2014). Swimming motility was assessed on 0.3% agar plates (3 g/l Bacto agar [Becton Dickinson] and 8 g/l Nutrient Broth [Becton Dickinson]). Overnight cultures grown at 37°C and 200 rpm in LB were point inoculated on the plates by depositing 1  $\mu\text{l}$  of culture directly into the agar in the center of the plate. Plates were incubated face up at 37°C, and the swim diameter (in centimeters) was measured after at 16 h.

Swarming motility was assessed on 0.6% agar plates (6 g/l Bacto agar [Becton Dickinson], 5 g Bacto-peptone [Becton Dickinson], 3 g/l Yeast Extract [Sigma], and 5 g/l D. glucose). Overnight cultures grown at 37°C and 200 rpm in LB were point inoculated on the plates by depositing 1  $\mu\text{l}$  of culture directly into the agar in the center of the plate. Plates were incubated face up at 37°C, and the swarming motility was examined after 16 h.

Twitching motility was assessed on 1.5% agar LB plates. Overnight cultures (37°C, 200 rpm; LB) were used to inoculate twitch plates by depositing 1  $\mu\text{l}$  of culture directly into agar in the bottom of the plate. Plates were incubated face down at 37°C for 16 h, and the twitching motility visualized by fixing the culture with Water : Glacial acetic Acid : Methanol at a ratio of 4 : 1 : 5 (v/v) and stained with 0.1% crystal violet.

## Pyoverdine Quantification

*Pseudomonas aeruginosa* PAO1 were cultivated in 37°C in Iron-depleted succinate medium (1 /L, 7.86 g  $\text{K}_2\text{HPO}_4 \cdot 3\text{H}_2\text{O}$ , 3 g  $\text{KH}_2\text{PO}_4$ , 1 g  $(\text{NH}_4)_2\text{SO}_4$ ; 0.1 g  $\text{MgSO}_4 \cdot 7\text{H}_2\text{O}$ ; 4 g succinate; PH = 7.0) (Stintzi et al., 1998). The OD600 was recorded after 24 h culture using NanoDrop 2000 spectrophotometer (Thermo Fisher Scientific). Cell-free supernatant was collected by max speed centrifuged and measured at A404 was recorded using succinate medium as a blank.

## Pyocyanin Quantification

Pyocyanin was assayed from *P. aeruginosa* PAO1 cultured in LB medium overnight at 37°C and 250 rpm. Single colony was inoculated into 5 mL culture for 16 h. The 5 mL culture were centrifuged at 12,000  $\times$  g for 5 min and the cell free supernatants mixed with equal volume of chloroform followed by continuous rocking for 30 min at room temperature. The solvent phase was obtained by brief centrifugation, mixed with 5 mL 0.2 mol / L HCl, and rocked at room temperature for an additional 30 min (Filloux and Ramos, 2014). The pyocyanin quantification was determined by measuring absorbance of supernatant at A520 nm and normalizing against the cell density at OD600.

## Elastase Quantification

Elastase production in *P. aeruginosa* strains were performed by Elastin-Congo Red (Sigma) assay (Lee et al., 2013). Single colonies of the *P. aeruginosa* strains were inoculated into 10 mL LB and cultured for 16 h at 37°C and 250 rpm. The cultures were centrifuged at 12,000  $\times$  g for 5 min to obtain cell-free supernatant. Briefly, 500  $\mu\text{L}$  of bacterial cell-free supernatant was mixed with an equal volume of 5 mg/mL elastin-Congo red with ECR buffer in 2 mL Eppendorf tube and incubated at 37°C shaker for 2 h. The quantity of Congo red dye released from the elastin digestion is proportional to the amount of elastase in the supernatant. Elastase quantification was determined using a spectrophotometer at A520 and normalized against the cell density at OD600.

## Biofilm Formation Assay and Quantification

Biofilm formation was assayed by 96-well plates as previously described (Filloux and Ramos, 2014). A single colony was inoculated into 10 mL LB broth and grown at 37°C, 200 rpm overnight. OD600 was measured by NanoDrop spectrophotometer and the culture was diluted to OD600 = 0.5. A volume of 1  $\mu\text{L}$  diluted cells was added to 200  $\mu\text{L}$  LB medium in sterile 96 well plate incubate at 37°C statically for 16 h. The plate was washed with Ultra-pure water at least 3 times and stained with 250  $\mu\text{L}$  0.1 % crystal violet for 15 min. The plate was rinsed, dried at room temperature, and the remaining dye was solubilized with 300  $\mu\text{L}$  Dimethyl sulfoxide (DMSO). The dissolved biofilm was measured by the spectrophotometer at absorbance A550.

## Quorum Sensing Signal Extraction and Quantification

Quorum sensing signal extraction was conducted as previously described by Dong et al. (2008). Single colonies of the *P. aeruginosa* cells were inoculated into 5 mL LB broth and grown overnight at 37°C and 200 rpm. The signals were extracted from 5 mL of supernatants with an equal volume of acidified ethyl acetate (0.1% Acetic acid) twice. The organic phase was transfer to a fresh tube and dried with nitrogen gas. The extracted compounds were dissolved in 1 mL filtered HPLC grade methanol for LC-MS analysis.

The LC-MS method was adapted from the Nishaben M. Patel method (Patel et al., 2016). HPLC was performed on a

Dionex Ultimate 3000 system (Thermo Fisher Scientific) using a C18 reverse-phase column (Thermo Fisher Scientific) and varying concentration gradients of methanol and consisted of 0.1% acidified water as mobile phase. The gradient profile for chromatography was as follows: 2% methanol and 98% water for 1.5 min, linear increase in methanol to 100% over 5 min, isocratic 100% methanol for 4 min, and then equilibration with 2% methanol and 98% water for 1.5 min. The flow rate was constant at 0.4 mL/min.

Compounds separated by HPLC were detected by heated electrospray ionization coupled to high-resolution mass spectroscopy (HESI-MS, Q Exactive Focus, Thermo Fisher Scientific). The analysis was performed under positive ionization mode. Settings for the ion source were: 10 aux gas flow rate, 40 sheath gas flow rate, 0 sweep gas flow rate, 4 kV spray voltage, 320°C capillary temperature, 350°C heater temperature, and 50 S-lens RF level. Nitrogen was used as a nebulizing gas by the ion trap source. The MS/MS method was designed to perform an MS1 full-scan (100 to 1,000 m/z, no fragmentation) together with the SIM model. Settings for the SIM method were 35,000 resolution, 1.0 m/z isolation offset, 4.0 isolation window, and centroid spectrum. Signals mass scans were set 3OC12HSL at 298.20128 m/z, C4HSL at 172.09682 m/z, PQS at 260.1645 m/z, respectively. Data analysis was performed using the Thermo Xcalibur software (Thermo Fisher Scientific) and TraceFinder (Thermo Fisher Scientific).

## RNA Purification and qPCR Analysis

Overnight cultures of *P. aeruginosa* PAO1 were diluted in LB broth and incubated at 37°C to OD<sub>600</sub> = 1.0. Bacterial pellets were obtained by centrifugation at 4°C for 3 min at 12,000 × g. Total RNA samples were purified using the RNeasy miniprep kit (Z3741, Promega) following the manufacturers' instruction. Genomic DNA was digested by using the TURBO DNA-free Kit (AM1907, Thermo Fisher Scientific) and the integrity and purity of the RNA determined by NanoDrop and gel electrophoresis. cDNA was generated by using FastKing RT Kit (KR116, Tiangen, China) and Real-time qPCR was carried out using PowerUp™ SYBR™ Green Master Mix (A25742, Applied Biosystems™) in the QuantStudio™ 6 Flex Real-Time PCR System (Applied Biosystems™). The *proC* and *rpoD* were used as house-keeping genes. The primer specific to the original copy of genes is listed in Supplementary Table 2.

## Data Analysis

Experimental data are expressed as means ± standard error. Significance was determined using one-way ANOVA analysis of variance with Tukey HSD multiple comparisons in Python (version 3.7). A *P* value of <0.05 was considered significant. The alphabet (a, b, ab, cd, bd, etc.) on the plot represents the statistically significant difference. The same alphabet on the data points signifies no significant differences between the data points. Different alphabets on the data points signify significant differences between those points. More than one alphabet on one strain means it across two or more groups. Plots were generated by R (version 3.6.0).

## Accession Number(s)

This Whole Genome Sequence project has been deposited at NCBI under the BioProject accession number PRJNA596099. Biosample accession number SAMN13612472, SAMN13612473, SAMN13612474, SAMN13612475, SAMN13612476. RefSeq accession number GCF\_013305845.1, GCF\_013350345.1, GCF\_013305815.1, GCF\_013350355.1, GCF\_013305765.1. SRA accession number SRX7885129, SRX7885172, SRX7885130, SRX7885131, SRX7885173, SRS6294844, SRX7885133, SRX7874733.

## RESULTS

### PAO1 Sublines Produce Different Levels of Quorum Sensing Signals and Quorum Sensing-Associated Virulence Factors

Phenotypic variations among the laboratory strains of *P. aeruginosa* PAO1 have been attributed to microevolution of strains during culture in selective media or prolonged passage in the laboratory (Klockgether et al., 2010; Chandler et al., 2019). Due to the immense influence of microevolution on the repeatability of research work, particularly in the field of QS, we investigated the impact of such mutations on the production of QS signals and QS associated virulence factors in 5 PAO1 sublines from our lab collection (Table 1 and Supplementary Table 1). We examined the production of the QS signals, 3OC12HSL, PQS, and C4HSL in the PAO1 sublines using LC-MS analysis. The production of the QS signals was not consistent across the 5 sublines. The highest amount of 3OC12HSL was produced by PAO1-B and PAO1-E followed by similar levels in PAO1-C and PAO1-D (Figure 1A). On the other hand, PAO1-C and PAO1-D produced the highest level of C4HSL compared to the other three sublines (Figure 1B). No significant difference in PQS production was observed in the three sublines, PAO1-B, C, and D (Figure 1C). The subline PAO1-A was found to produce the least amount of all three QS signals, with trace amounts of 3OC12HSL detected in our analysis (Figure 1). Consistently, the relative expression levels of the QS regulators genes in PAO1-A in comparison with PAO1-E correlated well with the production of their cognate QS signals (Supplementary Figure 2).

Elastase, encoded by *lasB*, relies on the *las* QS system. Elastase has tissue-damaging and proteinase inhibiting activity and targets plasma proteins such as immunoglobulins, coagulation, and complement factors (Pearson et al., 1997). Across the 5 sublines, PAO1-D produced the highest amount of elastase. However, this was not significantly greater than the amount produced by PAO1-C (Figure 1D). Intriguingly, PAO1-A produced similar amounts of elastase as PAO1-B and PAO1-E despite its low QS signal production (Figure 1D).

Pyocyanin is an evolutionarily conserved virulence factor crucial for *P. aeruginosa* lung infection. Pyocyanin is regulated by the *pqs* and *rhl* QS systems, and its production is exacerbated in *lasR* mutants under phosphate depleted condition (Lau et al., 2004). Quantification of pyocyanin production revealed marked differences in levels across the 5 sublines. PAO1-C and PAO1-D

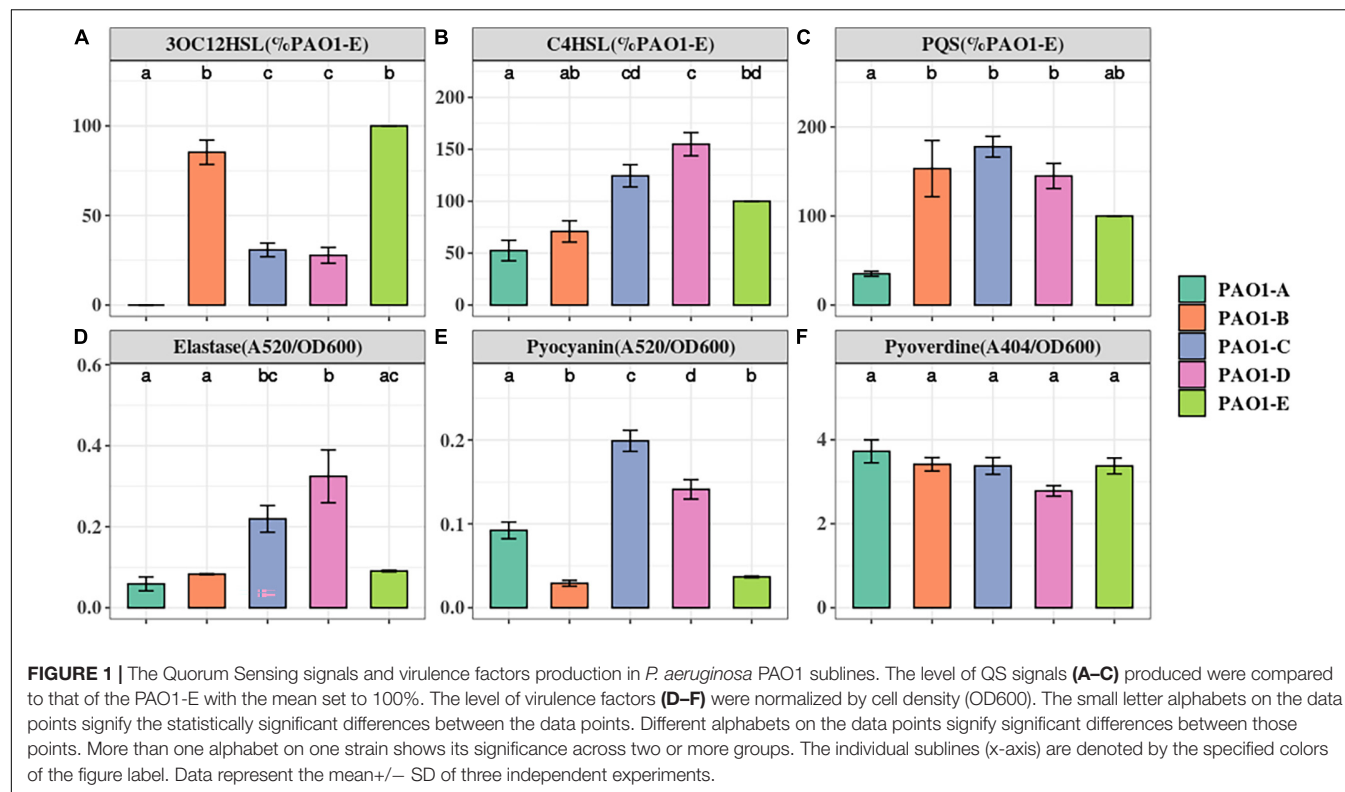


**FIGURE 1 |** The Quorum Sensing signals and virulence factors production in *P. aeruginosa* PAO1 sublines. The level of QS signals (**A–C**) produced were compared to that of the PAO1-E with the mean set to 100%. The level of virulence factors (**D–F**) were normalized by cell density (OD600). The small letter alphabets on the data points signify the statistically significant differences between the data points. Different alphabets on the data points signify significant differences between those points. More than one alphabet on one strain shows its significance across two or more groups. The individual sublines (x-axis) are denoted by the specified colors of the figure label. Data represent the mean $\pm$  SD of three independent experiments.

produced significantly greater levels of pyocyanin compared to PAO1-B and PAO1-E (Figure 1E). PAO1-A produce pyocyanin but significantly less compared to the PAO1-C/D (Figure 1E).

Pyoverdine, the main siderophore produced by *P. aeruginosa*, is regulated by QS and is a major contributor to colonization and establishing infections (Ravel and Cornelis, 2003). The result shows no significant changes in the production of the siderophore among the other 5 sublines (Figure 1F).

## Differences in Biofilm Formation and Motility Among the PAO1 Sublines

Biofilm is a common adaptive state of *P. aeruginosa* which confers antibiotic resistance, enhances evasion of host immune responses, and permits persistent infections (Costerton et al., 1999; Gellatly and Hancock, 2013). Biofilm formation of the 5 PAO1 sublines was assayed using 96-well plates after a 16-h static culture. From our biofilm assay, we observed different levels of biofilm formation across the sublines with significantly higher levels occurring in PAO1-B and PAO1-E compared with the other 3 sublines (Figure 2A).

Swimming motility which is mediated by flagella was not affected by the mutations in the sublines as no significant differences were observed across the sublines (Figure 2B). However, different swarming phenotypes were observed among the strains (Figure 2C). PAO1-D, followed by PAO1-C, swarmed with the largest diameter, whereas PAO1-B and PAO1-E displayed the least swarming motility (Figure 2C).

Pili formation is vital for adhesion, motility, DNA uptake, and biofilm formation (Barken et al., 2008). From our assay,

pili-mediated twitching motility was inconsistent among some of the sublines. PAO1-D exhibited the highest twitching motility followed by PAO1-A. Almost similar levels of twitching were observed in PAO1-B and PAO1-C which were slightly different in comparison to PAO1-E (Figure 2C).

## Genomic Variation Among PAO1 Sublines

To identify the underlying mutations accounting for the discrepancies in QS associated phenotypes across the 5 PAO1 sublines, we employed High-Throughput Whole Genome Sequencing (WGS) using Illumina PE-150 and Nanopore technology. The details of the whole genome sequence data of the selected *P. aeruginosa* PAO1 sublines are summarized in Table 1. The genomes of the strains were analyzed using both reference-guided mapping and *de novo* assembly approach (Supplementary Figure 1), coupled with mapping and assembly based callers for maximum variation detection.

A total of 230 SNPs and short indels was shared among the 5 sublines (Figure 3). The detailed information of SNPs and short indels in each subline relative to the reference sequence is summarized in Table 2. Six SNPs and short indels were identified in PAO1-A genome, an 18 bp deletion in the region of *mexT*, a synonymous variant in PA0020, two resulting in missense variants of PA1975 and PA3191, one in the non-coding sequence between *psdR-dppA3* intergenic region, and one disruptive 3 bp in-frame insertion of TCG in sequence for the autoinducer binding domain in *LasR*, which regulates the *las*

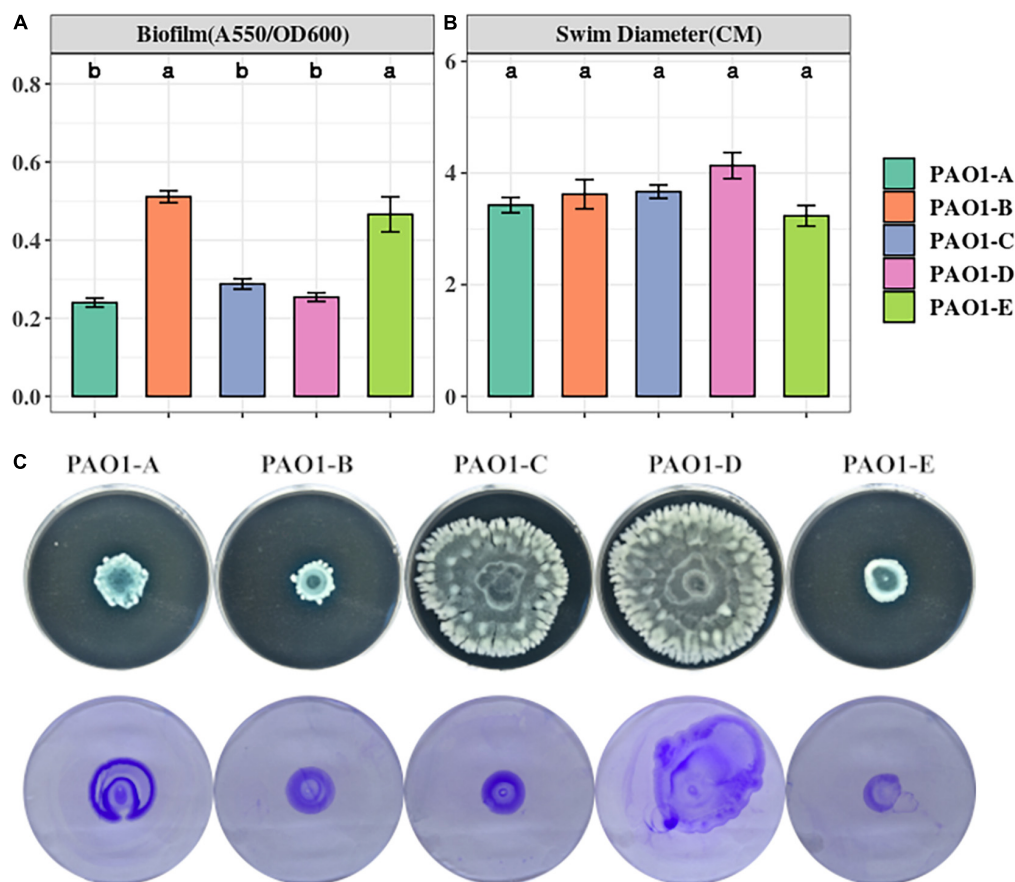


**FIGURE 2 | (A)** Biofilm formation was assayed from 16-h LB cultures in 96 well plates. The data represent mean $\pm$  SD of six independent biofilm assays. **(B)** Swimming motility of the sublines ( $n = 3$ ). **(C)** Swarming (top) and twitching (bottom) motility was assayed on LB medium incubated for 16 h ( $n = 3$ ).

QS system (Heurlier et al., 2005; **Table 2**). PAO1-B and PAO1-C shared common SNPs resulting in a missense variant of the aminoacyl-tRNA biosynthesis gene, PA4277.2. Additionally, the PAO1-C subline contained the other two SNPs, one resulting in a synonymous variant in PA3316 and the other present in the non-coding region between *psdR* and *dppA3*. The latter was also identified in the PAO1-C and PAO1-D sublines (**Table 2**). Five other SNPs and short indels were identified in the PAO1-D genome, two synonymous variants located in *leuB* and PA0020, and another two as missense variants in *htpG* and PA3637 sequence, in addition to the intergenic region of *psdR* and *dppA3* (**Table 2**), also an 18 bp deletion in *mexT* that is consistent with indel in PAO1-A. No unique SNPs were identified in the subline PAO1-E.

Using comparative genomic analysis, we identified 3 structural variations (SVs), among which two were present in the 5 sublines (**Table 3**). These include tandem repeats or copy number variations (CNVs) occurring from PA0717-PA0727 genomic region and deletion in PA4684/PA4685 region from 5,253,693 to 5,243,687 (**Table 3**). The PA0717-PA0727 cluster is annotated as a bacteriophage Pf1-like hypothetical protein (Hill et al., 1991), whereas PA4684 and PA4685 encode hypothetical proteins and form an operon with PA4686. These two variations

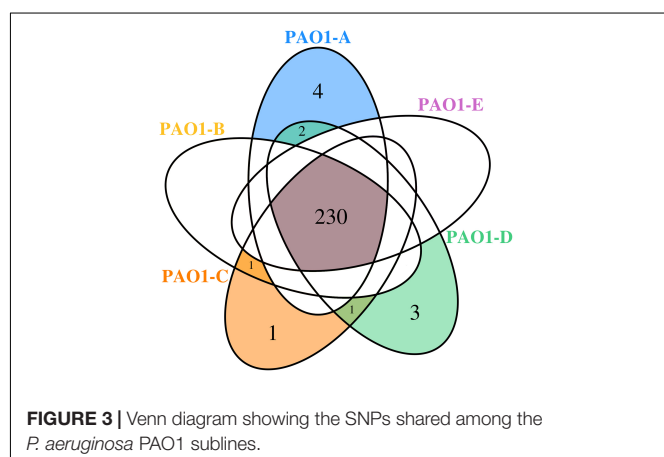


**FIGURE 3 |** Venn diagram showing the SNPs shared among the *P. aeruginosa* PAO1 sublines.

in the PA0717-PA0727 genomic region and the deletion in PA4684/PA4685 region were also detected in *P. aeruginosa* PAO1-DSM (Davies and Davies, 2010), and *P. aeruginosa* isolates PA14 (Klockgether et al., 2011). One unique SV detected in PAO1-C sublines was due to 8,384 bp deletion in the region containing genes of the *mexT*, Resistance-Nodulation-Cell

**TABLE 2 |** List of individual SNPs in each subline.

Category	Position	Locus	REF	ALT	SNP type	Encoded product
PAO1-A/PAO1-D	22278	PA0020	C	T	synonymous_variant	T4P secretin-associated protein TsaP
PAO1-A/PAO1-D	2807724	PA2492	GCGCTGTCGCGCCTGCGCA	G	disruptive_inframe_deletion	transcriptional regulator MexT
PAO1-B/PAO1-C	4785702	PA4277.2	G	A	missense_variant	tRNA-Gly
PAO1-A	1558324	PA1430	A	ATCG	disruptive_inframe_insertion	transcriptional regulator LasR
PAO1-A	2160063	PA1975	T	G	missense_variant	hypothetical protein
PAO1-A	3582640	PA3191	C	A	missense_variant	glucose transport sensor GtrS
PAO1-A	5036907	Interg. (PA4499–PA4500)	C	G		PdsR-DppA3
PAO1-C	5036884	Interg. (PA4499–PA4500)	C	T		PdsR-DppA3
PAO1-C	3823424	PA3316	C	T	synonymous_variant	probable permease of ABC transporter
PAO1-D	5036884	Interg. (PA4499–PA4500)	C	A		PdsR-DppA3
PAO1-D	1737560	PA1596	A	G	missense_variant	heat shock protein HtpG
PAO1-D	3500812	PA3118	C	A	synonymous_variant	3-isopropylmalate dehydrogenase
PAO1-D	4118004	PA3676	C	G	missense_variant	MexK

ALT represent sublines genotype. PAO1-E is devoid of individual SNPs from whole genomic sequence.

**TABLE 3 |** List of structure variation in each subline.

Category	Start position	End position	Len(bp)	Locus	SVs type	Encoded product
SVs in all sublines	5253693	5254687	994	PA4684/PA4685	DEL	hypothetical protein
	789150	795774	6624	PA0717-PA0727	CNV	hypothetical protein of bacteriophage Pf1
SV in PAO1-C only	2808156	2816540	8384	mexT/mexE/mexF oprN/PA2496/PA2497/PA2498	DEL	Resistance-Nodulation-Cell Division multidrug efflux

diversion (RND) multidrug efflux (*mexE*, *mexF*, and *oprN*), and the downstream genes, PA2496, PA2497, and PA2498 (Table 3). This deletion in PAO1-C is located downstream of *mexT*. Also, a short indel of 18 bp was identified in both PAO1-A and PAO1-D genome in the coding sequence for the transcriptional regulator MexT (RND multidrug efflux), resulted in disruptive in-frame deletion.

### The Short Indel of *lasR* and *mexT* Affect Quorum Sensing in *Pseudomonas aeruginosa* PAO1

Mutations in *mexT* and *lasR* are commonly reported in clinical isolates and have been recently reported in lab strains and clinical isolates (Köhler et al., 2001; Sobel et al., 2005; Klockgether et al., 2010; Kostylev et al., 2019). The *lasR* mutants have been associated with chronic infections and increased fitness under specific metabolic stress conditions (Köhler et al., 2009). The *mexT* mutations are also known to be induced by growth in the presence of antibiotics (Sobel et al., 2005), and are associated with the regulation of most QS factors and fitness of *P. aeruginosa* strains (Kostylev et al., 2019). To further investigate the impact of the MexT and LasR on the variation of QS associated traits among the sublines, we introduced the 18 bp *mexT* mutations found in PAO1-A and PAO1-D into the *mexT* of PAO1-E resulting in the strain PAO1-EΔ*mexT*. Additionally, we introduced the 3 bp insertion in *lasR* of PAO1-A into PAO1-E to obtain the strain PAO1-EΔ*lasR*. The PAO1-EΔ*mexT* produced a significantly decreased level of 3OC12HSL but an

increased level of C4HSL production compared to the parent strain (Figures 4A,B). PQS production was not significantly different between PAO1-E and PAO1-EΔ*mexT* (Figure 4C). Conversely, in PAO1-EΔ*lasR*, the production of 3OC12HSL, C4HSL, and PQS significantly decreased in comparison with the PAO1-E (Figure 4). Additionally, in PAO1-EΔ*mexT* elastase and pyocyanin production levels were significantly greater than that of the parental subline PAO1-E whereas their levels significantly decreased in the PAO1-EΔ*lasR* (Figures 4D,E).

Both PAO1-EΔ*mexT* and PAO1-EΔ*lasR* produced less biofilm compared to PAO1-E; however, a much significant decrease in biofilm was observed in the *lasR* mutant compared to the *mexT* mutant (Figure 4F). Although the 3 bp *lasR* insertion had little effect on swarming, the 18 bp deletion in *mexT* significantly increased the swarming motility in PAO1-E (Figure 4G). The introduction of the *mexT* mutations in the PAO1-E resulted in increased twitching motility; however, no significant difference in twitching was observed in the parent strain and the PAO1-EΔ*lasR* (Figure 4G).

### Evolution of *mexT* and *lasR* in *Pseudomonas aeruginosa*

Based on the frequency of *lasR* and *mexT* mutations and their influence on the fitness of *P. aeruginosa* strains (Feltner et al., 2016; Oshri et al., 2018; Kostylev et al., 2019; Clay et al., 2020), we decided to investigate the selective pressure driving *lasR* and *mexT* mutations in by calculating the substitution rates (nonsynonymous

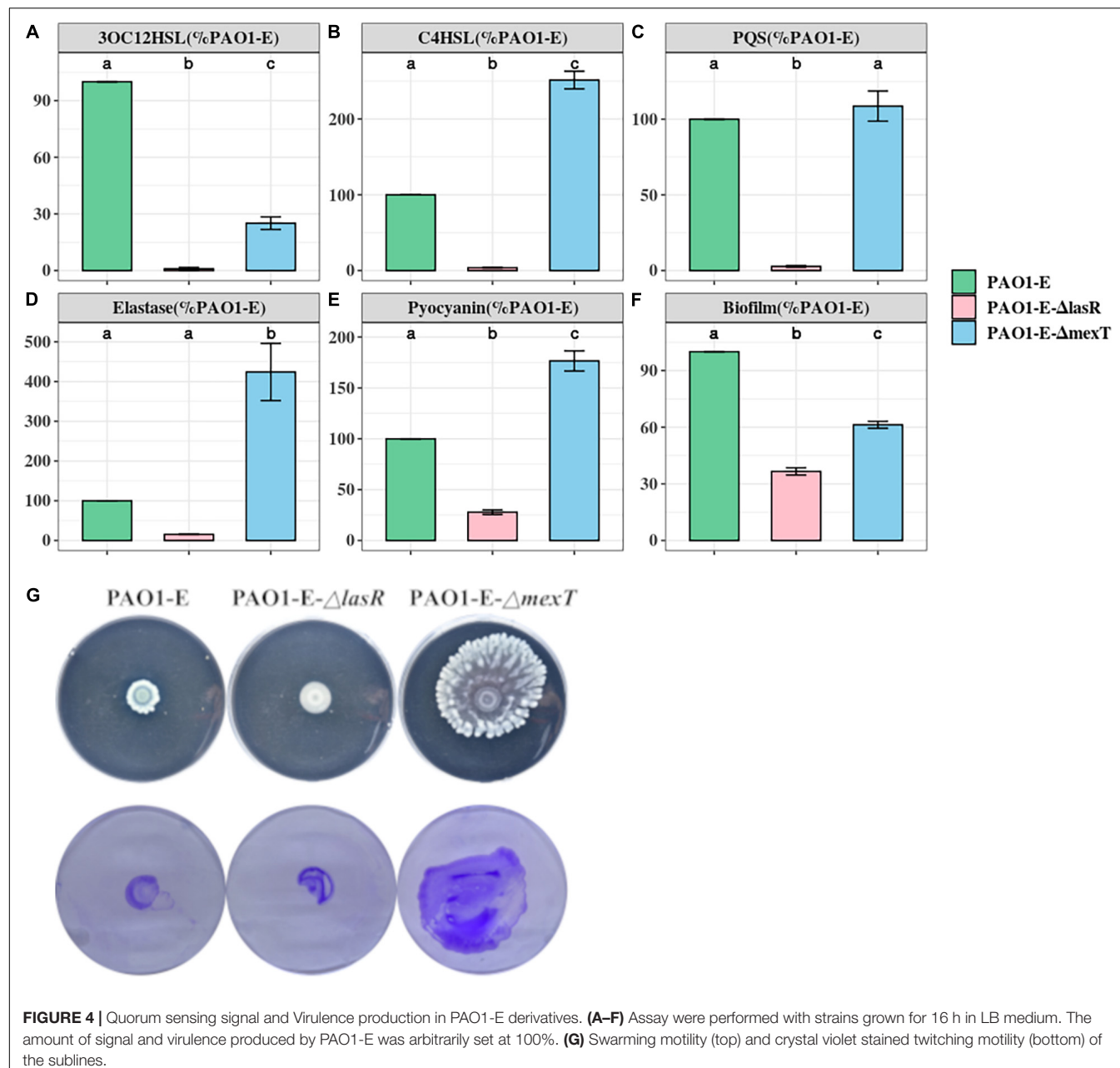


**FIGURE 4 |** Quorum sensing signal and Virulence production in PAO1-E derivatives. **(A–F)** Assay were performed with strains grown for 16 h in LB medium. The amount of signal and virulence produced by PAO1-E was arbitrarily set at 100%. **(G)** Swarming motility (top) and crystal violet stained twitching motility (bottom) of the sublines.

/synonymous [dN/dS]) of 4419 single-copy genes from 298 *P. aeruginosa* strains (see **Supplementary Material**) obtained for the Pseudomonas Genome Database (v18.1) (Winsor et al., 2016). From our analysis, we observed a higher nonsynonymous substitution rate for *lasR*, denoted by a higher dN/dS value (0.2881) in *lasR* compared to the other vital genes in quorum sensing signaling system (*pqsR*, *rhlI*, *rhlR*, *mexT*, *lasI*) in more than 4,000 single-copy genes (Third Quartile = 0.1145) (**Figure 5** and **Supplementary Table 3**). Although *mexT* is mutation-prone (Sobel et al., 2005), its low nonsynonymous substitution rates reflect a higher negative selection pressure (**Figure 5** and **Supplementary Table 3**).

For further estimation of the selection pressure and the mutation hot site, we performed the codon alignment of the 2,498 *lasR* sequences and 2,643 *mexT* sequences (see **Supplementary Material**) and calculated the dN/dS ratio of each site (**Figure 6** and **Supplementary Tables 5, 6**). Based on the mean posterior substitution rates, we observed that the LasR site shows more nonsynonymous mutation compared to the MexT in their amino acid sites (**Figure 6A** and **Supplementary Tables 5, 6**). In MexT, three distinct peaks at amino acid positions (17, 28, and 60) showed high mean posterior substitution rates of nonsynonymous (**Figure 6A** and **Supplementary Table 6**). These results also confirmed that the *mexT* undergoes high negative selection pressure.

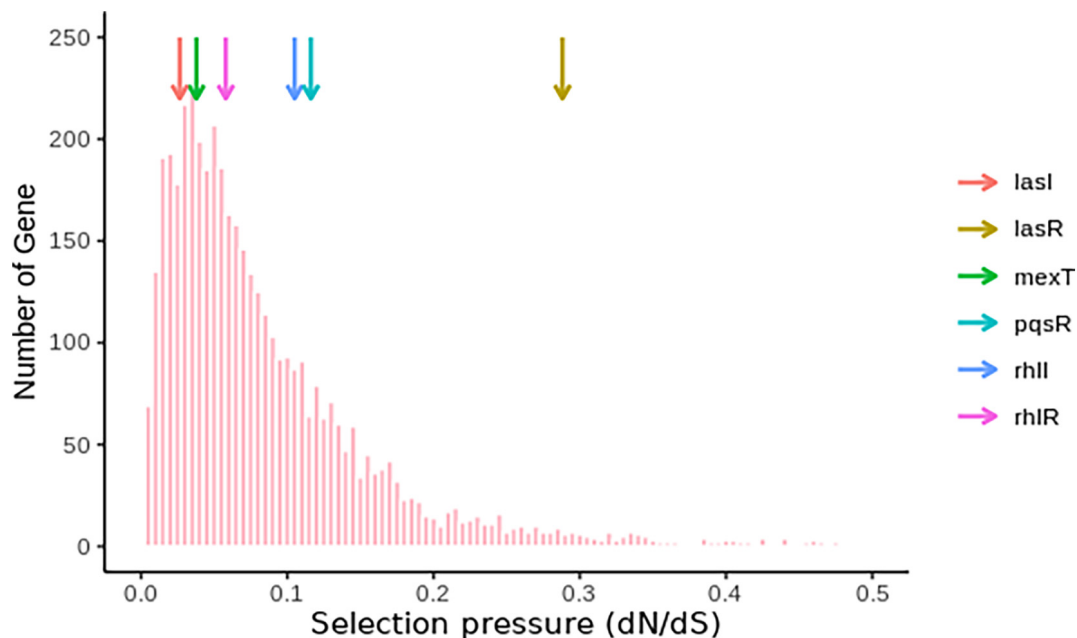


**FIGURE 5 |** Nucleotide substitution rates of single-copy genes in *P. aeruginosa*. The colored arrows show the positions of the genes and their respective dN/dS ratios.

We further investigated the nucleotide and amino acid insertion and deletion at each site of both the *lasR* and *mexT* sequences. Although the indel frequency of the *lasR* nucleotide sequences increased after 200 bp with an overall higher number of deletions than insertions, the distribution of insertion and deletion was even throughout the amino acid sequences of LasR (Figure 6B). For the *mexT* sequence, one indel-prone site (GCCGGCCAGCCGGCCA) was detected around 250 bp while the indel frequency in the amino acid sequences of *mexT* increased from the 5' to 3' (Figure 6C).

## DISCUSSION

In this study, we investigate the genetic and phenotypic variations of 5 *P. aeruginosa* PAO1 sublines. Previous in-house experimental analysis of QS signaling systems using the sublines from different lab members revealed inconsistencies prompting the investigation for underlying causes of microevolution occurring due to the continuous passage and maintenance of the sublines. Through a combination of molecular biology techniques and bioinformatics analysis, we show evidence for the implications for microevolution and further highlight the influence of the regulatory genes, *lasR* and *mexT*, which drive significant variations in QS-associated factors in the sublines. Since *P. aeruginosa* PAO1 is a model organism for QS research, the result from this study reveals how microevolution due to mutations in hot spots can account for possible inconsistencies in research data. This study also highlights the influence of the multi-drug efflux pump regulator, MexT, in regulating the QS system of *P. aeruginosa*. We show that MexT forms an intricate

QS regulatory pathway with the *lasR* regulator, where the loss of function mutation in *mexT* plays a compensatory role in the *lasR* mutant background (Figure 4) and enables the *lasR* mutants to produce QS-related virulence determinants. Our data adds to previous reports showing the role of MexT in rewiring the QS circuit of *P. aeruginosa* by influencing the regulation of virulence factors and fitness of the bacteria (Kostylev et al., 2019).

*Pseudomonas aeruginosa* strain PAO1 is one of the most widely used model organisms for QS research (Li et al., 2017). QS in *P. aeruginosa* regulates a vast majority of the physiological processes and virulence phenotypes (Ahator and Zhang, 2019), hence various research groups have focused on the development of anti-QS strategies as an alternative to combat the rising cases of antibiotic resistance in *P. aeruginosa*. However, most clinical isolates lose their QS functions via mutation in the key QS genes as well as mutation-prone genes (Hoffman et al., 2009), which makes the identification of anti-QS targets daunting. Additionally, the laboratory model organism, PAO1 from different research centers, has been shown to possess gene alterations such as SNPs and deletions in some mutation hotspots which underly their phenotypic variations and influence the repeatability of *P. aeruginosa* research (Klockgether et al., 2010; Hazen et al., 2016; Chandler et al., 2019; Lee et al., 2021). Among the frequently occurring mutations in both *P. aeruginosa* clinical isolates and laboratory strains are the *lasR* and *mexT* mutations which are vital for QS regulation, multidrug resistance, and drive adaptative processes in *P. aeruginosa* isolates to maximize their propagation during infection (Hazen et al., 2016; Winstanley et al., 2016).

Although previous studies have examined the genetic and phenotypic variations arising due to microevolution in lab

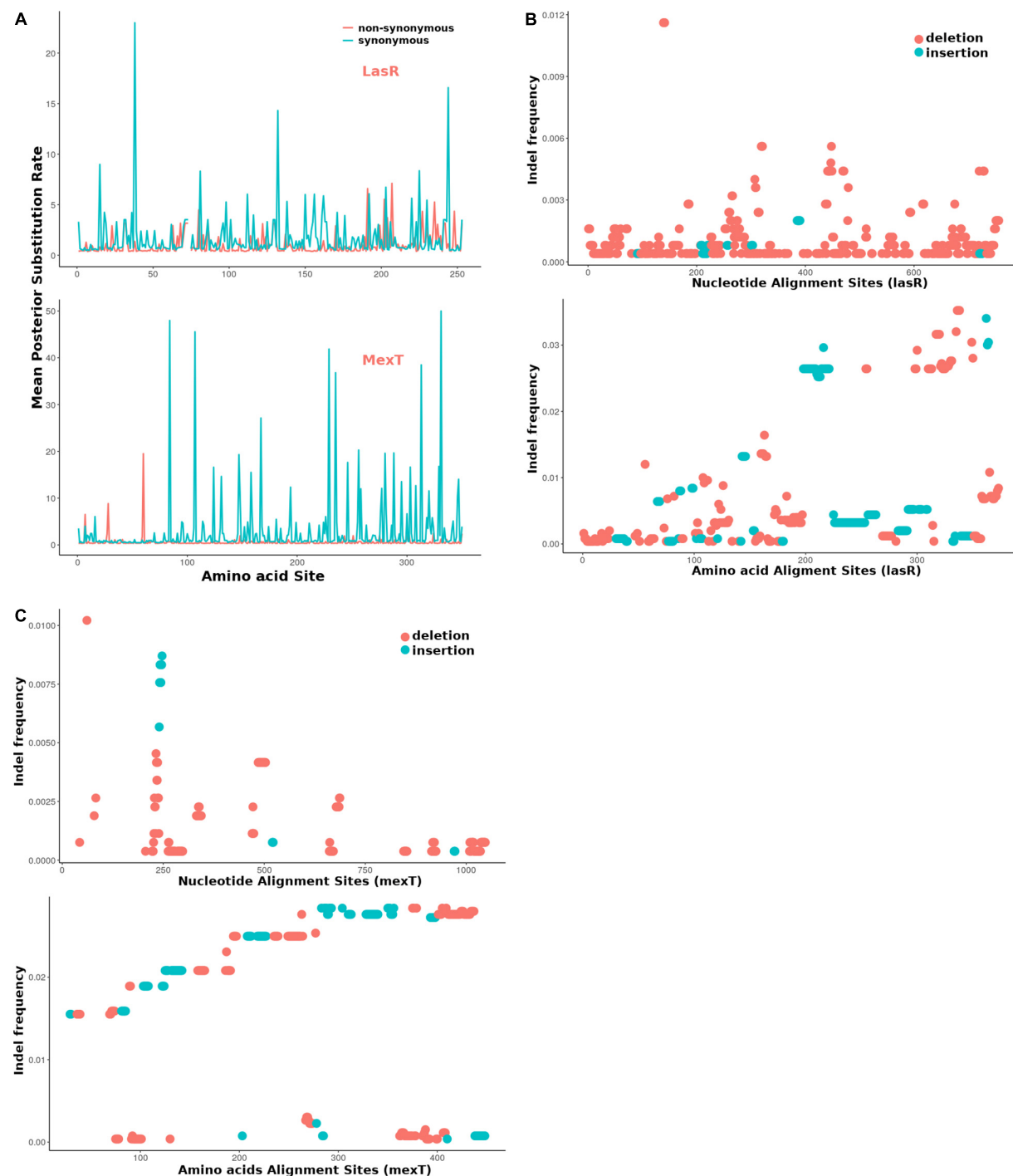


**FIGURE 6 |** The *mexT* and *lasR* sequence substitution rate in *P. aeruginosa*. **(A)** The nonsynonymous (orange peaks) and synonymous (green peaks) substitution rate in the amino acid sequences of LasR (top) and MexT (down). **(B)** The indel frequency of LasR nucleotides (up) and amino acid sequences (down) in *P. aeruginosa* strains. **(C)** The indel frequency of MexT nucleotides (up) and amino acid sequences (down) in *P. aeruginosa* strains. The deletion and insertion are indicated with orange and green dots.

strains of PAO1 sublines (Klockgether et al., 2010; Hazen et al., 2016; Chandler et al., 2019), they did not provide evidence of the underlying mutations driving the variations in QS

associated phenotypes, biofilm, motility, as well as other virulence determinants of the bacteria. To further understand the impact of these microevolution and the genetic basis for the variations

in phenotypes among the strains in our lab, we examined the mutations present in 5 sublines of *P. aeruginosa* PAO1 and their effect on QS and virulence. Our study used a combination of whole genome sequencing and molecular biology techniques to highlight the impact of minute gene alterations on QS and virulence among *P. aeruginosa* PAO1 sublines. Significantly, we further provide evidence that mutations in the transcriptional regulators, LasR and MexT, completely destabilize the QS circuit and account for the variations in the production of the PQS and C4HSL and their associated virulence factors among the sublines, thus indicating the significant impact of microevolution on the repeatability of QS and virulence studies using laboratory collections of PAO1.

MexT is a positive regulator of MexEF-OprN efflux pump and represses the outer membrane porin protein OprD (Köhler et al., 1999; Ochs et al., 1999; Sobel et al., 2005). From our analysis, *mexT* mutations were identified in two of the sublines with an additional subline containing deletion of the region containing the *mexT* and *mexEF oprN* cluster as well as the PA2496, PA2497, and PA2498. The *mexT* mutations have been reported in other studies of clinical and lab strains (Sobel et al., 2005; Quale et al., 2006; Walsh and Amyes, 2007; Klockgether et al., 2010; Poonsuk et al., 2014; Chandler et al., 2019). In support, recent work showed MexT as a factor that reorganizes the QS system in *P. aeruginosa* independent of *lasR* and is therefore vital for the fitness of the bacteria (Kostylev et al., 2019). This in part can be due to the function of the MexEF-OprN in transporting of homoserine lactones and influence on cell-cell signaling (Köhler et al., 2001).

MexT mutations could promote pleiotropic effects on the cell as it influences the expression of at least 40 genes (Tian et al., 2009a). Accordingly, by introducing the 18 bp *mexT* mutation in the PAO1-E subline, we observed significant changes in QS signal production as well as pyocyanin, elastase, biofilm formation, and motility. Based on our data, we believe that MexT may have an opposing role to LasR and may thus serve a compensatory mutation for *lasR* mutants or vice versa. PAO1-A had both *lasR* and *mexT* mutations with a characteristic loss on 3OC12HSL production but did not lose its ability to produce virulence factors such as pyocyanin, elastase, and pyoverdine (Figure 4). Thus, a combination of *mexT* and *lasR* mutations does not drive the bacteria toward a non-virulent state as compared to *lasR* mutations alone. As such despite producing the least levels of QS signals with almost no 3OC12HSL, PAO1-A still produced virulence factors and formed biofilms and maintained its motility morphology comparable to the other sublines (Figures 1, 2, 4).

In support of the above observation, we note that mutation of *lasR* alone decreased the production of pyocyanin in the PAO1-E which was contrary to *mexT* mutations in the same subline. Pyocyanin is regulated in a *las*-independently manner by the *pqs* and *rhl* systems. Also, despite the defective *las* system, elastase production was comparable among PAO1-A, PAO1-B, and PAO1-E. Although the *las* system regulates elastase production (Rust et al., 1996), the defective *las* system in PAO1-A did not cause a significant loss in elastase production. Hence it is highly possible that the defective *las* system coupled with the *mexT* mutation may account for the increase in pyocyanin and elastase production in PAO1-A. This in part could be due to the

independent regulation of the *pqs* and *rhl* systems or the effect of *mexT* mutation.

Due to the importance of motility for promoting infections, colonization, and initializing biofilm formation on both biotic and abiotic surfaces (O'Toole and Kolter, 1998), the differences in motility observed in the sublines will greatly impact their level of pathogenicity. Another interesting observation in the interplay of *mexT* and *lasR* is the control of twitching and swarming motility. The high levels of twitching and swarming observed in the sublines, PAO1-C, PAO1-D, and PAO1-EΔ*mexT* containing *mexT* mutations affirms the negative regulation of MexT on pili formation and flagellar mediated motility (Tian et al., 2009b). Twitching is influenced by type IV pili whereas swarming is influenced by both flagellar and type IV pili (Mattick, 2002; Breidenstein et al., 2011; Taguchi and Ichinose, 2011; Ichinose et al., 2016). Accordingly, we believe that the increase in twitching motility in PAO1-D compared to PAO1-E is due to *mexT* mutation. Although the *las* QS system does not regulate twitching motility (Beatson et al., 2002; Burrows, 2012), certain factors such rhamnolipids which influence motility are regulated by the *las* system (Pearson et al., 1997; Köhler et al., 2001; Tian et al., 2009b). In the defective *lasR* and *mexT* in PAO1-A, we observe a slight increase in twitching and swarming above those of the PAO1-B and PAO1-E sublines. Also, as MexT regulation of twitching motility could be dependent or independent of MexEF-OprN (Tian et al., 2009b), we believe that the deletion of the *mexT*, *mexEF oprN* gene cluster could account for the loss of twitching motility in the PAO1-C.

This work presents fascinating information about alternative pathways that compensate for loss of QS mediated functions and highlights the role of MexT in reorganizing the QS system in the bacteria. In the context of *lasR* and *mexT* regulation, *mexT* tends to alleviate the loss of QS associated virulence caused by *lasR* defects which is particularly important for *P. aeruginosa* during the acute-chronic infection switch. The lower dN/dS (0.0378) in *mexT* in comparison to that of *lasR* and other single-copy genes (First Quartile = 0.0351) (Figures 5, 6) indicated the *mexT* is under higher selection pressure. It is possible that mutations occurring in *mexT* drive the bacterial toward a more virulent state which can be vital for the switch from avirulent to virulent phenotypes during the different stages of bacterial infections. The high synonymous substitution rates in the mutational hotspot, *mexT* strongly influences the phenotypes of *P. aeruginosa* PAO1 lineages (LoVullo and Schweizer, 2020), which show that mutations in *mexT* play a vital role in the fast evolutionary scenario in laboratory and clinical isolates. However, due to the high selection pressure on *mexT*, these mutations are eliminated and overlooked, making it difficult to identify the significance of *mexT* on the evolution time scale. Disentangling the short-term evolution of *mexT* on different lineage could offer an opportunity to understand pathogens with higher virulence on later infection patients.

Our study focused more on the genes that directly affect QS in *P. aeruginosa*, and the interaction between *lasR* and *mexT* still needs further investigation. Also mutations in genes such as *psdR* which influences the fitness of the bacteria and non-cooperative cheating in the presence of *lasR* mutants

(Asfahl et al., 2015; Kostylev et al., 2019) are currently being studied in our lab. Mutations in the intergenic region of transcriptional regulator, PsdR, has been shown to arise early in the evolution of *P. aeruginosa* strains growing in the presence of casein, and enhances fitness in the presence of *lasR* cheaters (Dandekar et al., 2012). DppA3 is a dipeptide binding protein with specificity for the transport of L-amino acids (Pletzer et al., 2014; Fernández et al., 2019). Derepression of this function of DppA3 by PsdR has been shown to enhance non-cooperative cheating in the *P. aeruginosa* population under QS-inducing conditions (Asfahl et al., 2015). As most of the regulatory systems in *P. aeruginosa* are highly coordinated and exhibit cross-talk, it may be a bit daunting to directly link phenotypes to specific microevolution events. Also, mutations in *lasR* and *mexT* occur during prolonged passage in special media and exposure to sub-inhibitory concentrations of antibiotics (Maseda et al., 2000; Hoffman et al., 2009), hence storage of laboratory collections of wild type PAO1 strains after prolonged passage or growth in the presence of such conditions should be avoided to minimize the microevolution of the strains. Understanding how these processes occur can help to address important problems in microbiology by explaining observed differences in phenotypes, including virulence and resistance to antibiotics and the discrepancies in QS research.

## DATA AVAILABILITY STATEMENT

The datasets presented in this study can be found in online repositories. The names of the repository/repositories and

## REFERENCES

- Ahator, S. D., and Zhang, L. (2019). Small is mighty-chemical communication systems in *Pseudomonas aeruginosa*. *Annu. Rev. Microbiol.* 73, 559–578. doi: 10.1146/annurev-micro-020518-120044
- Andrews, S. (2010). *FastQC: A Quality Control Tool for High Throughput Sequence Data*. Available online at: <https://www.bioinformatics.babraham.ac.uk/> (accessed April 20, 2019).
- Asfahl, K. L., Walsh, J., Gilbert, K., and Schuster, M. (2015). Non-social adaptation defers a tragedy of the commons in *Pseudomonas aeruginosa* quorum sensing. *ISME J.* 9:1734. doi: 10.1038/ismej.2014.259
- Balasubramanian, D., Kumari, H., and Mathee, K. (2014). *Pseudomonas aeruginosa* AmpR: an acute-chronic switch regulator. *Pathog. Dis.* 73, 1–14. doi: 10.1111/1365-2409.12208
- Barken, K. B., Pamp, S. J., Yang, L., Gjermansen, M., Bertrand, J. J., Klausen, M., et al. (2008). Roles of type IV pili, flagellum-mediated motility and extracellular DNA in the formation of mature multicellular structures in *Pseudomonas aeruginosa* biofilms. *Environ. Microbiol.* 10, 2331–2343. doi: 10.1111/j.1462-2920.2008.01658.x
- Beatson, S. A., Whitchurch, C. B., Semmler, A. B. T., and Mattick, J. S. (2002). Quorum sensing is not required for twitching motility in *Pseudomonas aeruginosa*. *J. Bacteriol.* 184, 3598–3604. doi: 10.1128/JB.184.13.3598-3604.2002
- Breidenstein, E. B. M., de la Fuente-Núñez, C., and Hancock, R. E. W. (2011). *Pseudomonas aeruginosa*: all roads lead to resistance. *Trends Microbiol.* 19, 419–426. doi: 10.1016/j.tim.2011.04.005
- Burrows, L. L. (2012). *Pseudomonas aeruginosa* twitching motility: type IV Pili in action. *Annu. Rev. Microbiol.* 66, 493–520. doi: 10.1146/annurev-micro-092611-150055
- Bushnell, B. (2014). *Bbmap: A Fast, Accurate, Splice-Aware Aligner*. Available online at: <https://www.osti.gov/servlets/purl/1241166> (accessed August 18, 2019).
- Capella-Gutierrez, S., Silla-Martinez, J. M., and Gabaldon, T. (2009). trimAl: a tool for automated alignment trimming in large-scale phylogenetic analyses. *Bioinformatics* 25, 1972–1973. doi: 10.1093/bioinformatics/btp348
- Carmeli, Y., Troillet, N., Eliopoulos, G. M., and Samore, M. H. (1999). Emergence of antibiotic-resistant *Pseudomonas aeruginosa*: comparison of risks associated with different antipseudomonal agents. *Antimicrob. Agents Chemother.* 43, 1379–1382. doi: 10.1128/aac.43.6.1379
- Chakraborty, M., Vankuren, N. W., Zhao, R., Zhang, X., Kalsow, S., and Emerson, J. J. (2018). Hidden genetic variation shapes the structure of functional elements in *Drosophila*. *Nat. Genet.* 50, 20–25. doi: 10.1038/s41588-017-0010-y
- Chandler, C. E., Horspool, A. M., Hill, P. J., Wozniak, D. J., Schertzer, J. W., Rasko, D. A., et al. (2019). Genomic and phenotypic diversity among ten laboratory isolates of *Pseudomonas aeruginosa* PAO1. *J. Bacteriol.* 201:e00595-18. doi: 10.1128/JB.00595-18
- Chen, K., Wallis, J. W., McLellan, M. D., Larson, D. E., Kalicki, J. M., Pohl, C. S., et al. (2009). BreakDancer: an algorithm for high-resolution mapping of genomic structural variation. *Nat. Methods* 6, 677–681. doi: 10.1038/nmeth.1363
- Cingolani, P., Platts, A., Wang, L. L., Coon, M., Nguyen, T., Wang, L., et al. (2012). A program for annotating and predicting the effects of single nucleotide polymorphisms. *SnpEff. Fly (Austin)* 6, 80–92. doi: 10.4161/fly.19695
- Clay, M. E., Hammond, J. H., Zhong, F., Chen, X., Kowalski, C. H., Lee, A. J., et al. (2020). *Pseudomonas aeruginosa* lasR mutant fitness in microoxia is supported accession number(s) can be found below: <https://www.ncbi.nlm.nih.gov/bioproject/PRJNA596099>, PRJNA596099.

## AUTHOR CONTRIBUTIONS

YL, SA, XZ, and L-HZ designed the experiments. YL, SA, HW, and QF conducted the experiments. YL, YX, HW, and CL performed the data analysis. YL, SA, and L-HZ wrote the manuscript. XZ and YL conceived the study. All authors contributed to the article and approved the submitted version.

## FUNDING

This work was supported by the Natural Research Foundation of China (Grant No. 31330002), Key Projects of Guangzhou Science and Technology Plan (Grant No. 201804020066), Guangdong Technological Innovation Strategy of Special Funds (Grant No. 2018B020205003), and China Scholarship Council (CSC) (Grant 202008440425).

## SUPPLEMENTARY MATERIAL

The Supplementary Material for this article can be found online at: <https://www.frontiersin.org/articles/10.3389/fmicb.2022.821895/full#supplementary-material>

**Supplementary Script and Bioinformatic Data |** [https://github.com/lyonliuyang/P\\_aeruginosaPAO1\\_microevolution\\_Sup](https://github.com/lyonliuyang/P_aeruginosaPAO1_microevolution_Sup).

- by an Anr-regulated oxygen-binding hemerythrin. *Proc. Natl. Acad. Sci. U.S.A.* 117, 3167–3173. doi: 10.1073/pnas.1917576117
- Cordero, O. X., and Polz, M. F. (2014). Explaining microbial genomic diversity in light of evolutionary ecology. *Nat. Rev. Microbiol.* 12, 263–273. doi: 10.1038/nrmicro3218
- Costerton, J. W., Stewart, P. S., and Greenberg, E. P. (1999). Bacterial biofilms: a common cause of persistent infections. *Science* 284, 1318–1322. doi: 10.1126/science.284.5418.1318
- Dandekar, A. A., Chugani, S., and Greenberg, E. P. (2012). Bacterial quorum sensing and metabolic incentives to cooperate. *Science* 338, 264–266. doi: 10.1126/science.1227289
- Darling, A. E., Mau, B., and Perna, N. T. (2010). Progressivemauve: multiple genome alignment with gene gain, loss and rearrangement. *PLoS One* 5:e0011147. doi: 10.1371/journal.pone.0011147
- Davies, J., and Davies, D. (2010). Origins and evolution of antibiotic resistance. *Microbiol. Mol. Biol. Rev.* 74, 417–433. doi: 10.1128/MMBR.00016-10
- Depristo, M. A., Banks, E., Poplin, R., Garimella, K. V., Maguire, J. R., Hartl, C., et al. (2011). A framework for variation discovery and genotyping using next-generation DNA sequencing data. *Nat. Genet.* 43, 491–501. doi: 10.1038/ng.806
- Dong, Y., Zhang, X.-F., An, S.-W., Xu, J.-L., and Zhang, L.-H. (2008). A novel two-component system BqsS-BqsR modulates quorum sensing-dependent biofilm decay in *Pseudomonas aeruginosa*. *Commun. Integr. Biol.* 1, 88–96. doi: 10.4161/cib.1.1.6717
- Eickhoff, M. J., and Bassler, B. L. (2018). SnapShot: bacterial quorum sensing. *Cell* 174, 1328–1328.e1. doi: 10.1016/j.cell.2018.08.003
- Feltner, J. B., Wolter, D. J., Pope, C. E., Groleau, M. C., Smalley, N. E., Greenberg, E. P., et al. (2016). LasR variant cystic fibrosis isolates reveal an adaptable quorum-sensing hierarchy in *Pseudomonas aeruginosa*. *mBio* 7:eo1513–16. doi: 10.1128/mBio.01513-16
- Fernández, M., Rico-Jiménez, M., Ortega, Á, Daddaoua, A., García García, A. I., Martín-Mora, D., et al. (2019). Determination of ligand profiles for *Pseudomonas aeruginosa* solute binding proteins. *Int. J. Mol. Sci.* 20:5156. doi: 10.3390/ijms20205156
- Filloux, A., and Ramos, J. L. (2014). *Pseudomonas Methods and Protocols*. New York, NY: Springer, doi: 10.1007/978-1-4614-0473-0
- Gellatly, S. L., and Hancock, R. E. W. (2013). *Pseudomonas aeruginosa*: new insights into pathogenesis and host defenses. *Pathog. Dis.* 67, 159–173. doi: 10.1111/2049-632X.12033
- Hazen, T. H., Donnenberg, M. S., Panchalingam, S., Antonio, M., Hossain, A., Mandomando, I., et al. (2016). Genomic diversity of EPEC associated with clinical presentations of differing severity. *Nat. Microbiol.* 1:15014. doi: 10.1038/nmicrobiol.2015.14
- Heurlier, K., Haenni, M., Guy, L., Krishnapillai, V., and Haas, D. (2005). Quorum-sensing-negative (lasR) mutants of *Pseudomonas aeruginosa* avoid cell lysis and death. *J. Bacteriol.* 187, 4875–4883. doi: 10.1128/JB.187.14.4875
- Hill, D. F., Short, N. J., Perham, R. N., and Petersen, G. B. (1991). DNA sequence of the filamentous bacteriophage Pf1. *J. Mol. Biol.* 218, 349–364. doi: 10.1016/0022-2836(91)90717-K
- Hoffman, L. R., Kulasekara, H. D., Emerson, J., Houston, L. S., Burns, J. L., Ramsey, B. W., et al. (2009). *Pseudomonas aeruginosa* lasR mutants are associated with cystic fibrosis lung disease progression. *J. Cyst. Fibros.* 8, 66–70. doi: 10.1016/j.jcf.2008.09.006
- Horna, G., López, M., Guerra, H., Saénz, Y., and Ruiz, J. (2018). Interplay between MexAB-OprM and MexEF-OprN in clinical isolates of *Pseudomonas aeruginosa*. *Sci. Rep.* 8:16463. doi: 10.1038/s41598-018-34694-z
- Hussain, M., Liu, X., Tang, S., Zou, J., Wang, Z., Ali, Z., et al. (2022). Rapid detection of *Pseudomonas aeruginosa* based on lab-on-a-chip platform using immunomagnetic separation, light scattering, and machine learning. *Anal. Chim. Acta* 1189:339223. doi: 10.1016/j.aca.2021.339223
- Ichinose, Y., Sawada, T., Matsui, H., Yamamoto, M., Toyoda, K., Noutoshi, Y., et al. (2016). Motility-mediated regulation of virulence in *Pseudomonas syringae*. *Physiol. Mol. Plant Pathol.* 95, 50–54. doi: 10.1016/j.pmp.2016.02.005
- Jensen, V., Löns, D., Zaoui, C., Bredenbruch, F., Meissner, A., Dieterich, G., et al. (2006). RhlR expression in *Pseudomonas aeruginosa* is modulated by the *Pseudomonas* quinolone signal via PhoB-dependent and-independent pathways. *J. Bacteriol.* 188, 8601–8606. doi: 10.1128/JB.01378-06
- Juarez, P., Broutin, I., Bordi, C., Plésiat, P., and Llanes, C. (2018). Constitutive activation of MexT by amino acid substitutions results in MexEF-OprN overproduction in clinical isolates of *Pseudomonas aeruginosa*. *Antimicrob. Agents Chemother.* 62:e02445–17. doi: 10.1128/AAC.02445-17
- Katoh, K. (2002). MAFFT: a novel method for rapid multiple sequence alignment based on fast Fourier transform. *Nucleic Acids Res.* 30, 3059–3066. doi: 10.1093/nar/gkf436
- Klockgether, J., Cramer, N., Wiehmann, L., Davenport, C. F., and Tümler, B. (2011). *Pseudomonas aeruginosa* genomic structure and diversity. *Front. Microbiol.* 2:150. doi: 10.3389/fmicb.2011.00150
- Klockgether, J., Munder, A., Neugebauer, J., Davenport, C. F., Stanke, F., Larbig, K. D., et al. (2010). Genome diversity of *Pseudomonas aeruginosa* PAO1 laboratory strains. *J. Bacteriol.* 192, 1113–1121. doi: 10.1128/JB.01515-09
- Köhler, T., Buckling, A., and Van Delden, C. (2009). Cooperation and virulence of clinical *Pseudomonas aeruginosa* populations. *Proc. Natl. Acad. Sci. U.S.A.* 106, 6339–6344. doi: 10.1073/pnas.0811741106
- Köhler, T., Epp, S. F., Curty, L. K., and Pechère, J.-C. (1999). Characterization of MexT, the regulator of the MexE-MexF-OprN multidrug efflux system of *Pseudomonas aeruginosa*. *J. Bacteriol.* 181, 6300–6305. doi: 10.1128/JB.181.20.6300-6305.1999
- Köhler, T., Van Delden, C., Curty, L. K., Hamzehpour, M. M., and Pechère, J.-C. (2001). Overexpression of the MexEF-OprN multidrug efflux system affects cell-to-cell signaling in *Pseudomonas aeruginosa*. *J. Bacteriol.* 183, 5213–5222. doi: 10.1128/JB.183.18.5213-5222.2001
- Kostylev, M., Kim, D. Y., Smalley, N. E., Salukhe, I., Greenberg, E. P., and Dandekar, A. A. (2019). Evolution of the *Pseudomonas aeruginosa* quorum-sensing hierarchy. *Proc. Natl. Acad. Sci. U.S.A.* 116, 7027–7032. doi: 10.1073/pnas.1819796116
- Kurtz, S., Philippy, A., Delcher, A. L., Smoot, M., Shumway, M., Antonescu, C., et al. (2004). Versatile and open software for comparing large genomes. *Genome Biol.* 5:12. doi: 10.1186/gb-2004-5-2-r12
- Lau, G. W., Hassett, D. J., Ran, H., and Kong, F. (2004). The role of pyocyanin in *Pseudomonas aeruginosa* infection. *Trends Mol. Med.* 10, 599–606. doi: 10.1016/j.molmed.2004.10.002
- Lee, J., Wu, J., Deng, Y., Wang, J., Wang, C., Wang, J., et al. (2013). A cell-cell communication signal integrates quorum sensing and stress response. *Nat. Chem. Biol.* 9, 339–343. doi: 10.1038/nchembio.1225
- Lee, J., and Zhang, L. (2015). The hierarchy quorum sensing network in *Pseudomonas aeruginosa*. *Protein Cell* 6, 26–41. doi: 10.1007/s13238-014-0100-x
- Lee, S., Gallagher, L., and Manoil, C. (2021). Reconstructing a wild-type *Pseudomonas aeruginosa* reference strain PAO1. *J. Bacteriol.* 203:e0017921. doi: 10.1128/JB.00179-21
- Li, H. (2011). A statistical framework for SNP calling, mutation discovery, association mapping and population genetic parameter estimation from sequencing data. *Bioinformatics* 27, 2987–2993. doi: 10.1093/bioinformatics/btr509
- Li, H., and Durbin, R. (2009). Fast and accurate short read alignment with Burrows-Wheeler transform. *Bioinformatics* 25, 1754–1760. doi: 10.1093/bioinformatics/btp324
- Li, S., Duan, Y., Li, R., and Wang, X. (2017). Intracellular and extracellular biosynthesis of antibacterial silver nanoparticles by using *Pseudomonas aeruginosa*. *J. Nanosci. Nanotechnol.* 17, 9186–9191. doi: 10.1166/jnn.2017.13920
- LoVullo, E. D., and Schweizer, H. P. (2020). *Pseudomonas aeruginosa* mexT is an indicator of PAO1 strain integrity. *J. Med. Microbiol.* 69, 139–145. doi: 10.1099/jmm.0.001128
- Maseda, H., Saito, K., Nakajima, A., and Nakae, T. (2000). Variation of the mexT gene, a regulator of the MexEF-OprN efflux pump expression in wild-type strains of *Pseudomonas aeruginosa*. *FEMS Microbiol. Lett.* 192, 107–112. doi: 10.1016/S0378-1097(00)00419-5
- Mattick, J. S. (2002). Type IV pili and twitching motility. *Annu. Rev. Microbiol.* 56, 289–314. doi: 10.1146/annurev.micro.56.012302.160938
- Murrell, B., Moola, S., Mabona, A., Weighill, T., Sheward, D., Kosakovsky Pond, S. L., et al. (2013). FUBAR: a fast, unconstrained bayesian AppRoximation for inferring selection. *Mol. Biol. Evol.* 30, 1196–1205. doi: 10.1093/molbev/mst030
- Murrell, B., Weaver, S., Smith, M. D., Wertheim, J. O., Murrell, S., Aylward, A., et al. (2015). Gene-wide identification of episodic

- selection. *Mol. Biol. Evol.* 32, 1365–1371. doi: 10.1093/molbev/msv035
- Nguyen, L.-T., Schmidt, H. A., von Haeseler, A., and Minh, B. Q. (2015). IQ-TREE: a fast and effective stochastic algorithm for estimating maximum-likelihood phylogenies. *Mol. Biol. Evol.* 32, 268–274. doi: 10.1093/molbev/msu300
- Ochs, M. M., McCusker, M. P., Bains, M., and Hancock, R. E. W. (1999). Negative regulation of the *Pseudomonas aeruginosa* outer membrane porin OprD selective for imipenem and basic amino acids. *Antimicrob. Agents Chemother.* 43, 1085–1090. doi: 10.1128/AAC.43.5.1085
- Oshri, R. D., Zrihen, K. S., Shner, I., Bendori, S. O., and Eldar, A. (2018). Selection for increased quorum-sensing cooperation in *Pseudomonas aeruginosa* through the shut-down of a drug resistance pump. *ISME J.* 12, 2458–2469. doi: 10.1038/s41396-018-0205-y
- O'Toole, G. A., and Kolter, R. (1998). Flagellar and twitching motility are necessary for *Pseudomonas aeruginosa* biofilm development. *Mol. Microbiol.* 30, 295–304. doi: 10.1046/j.1365-2958.1998.01062.x
- Patel, N. M., Moore, J. D., Blackwell, H. E., and Amador-Noguez, D. (2016). Identification of unanticipated and novel N-acyl L-homoserine lactones (AHLs) using a sensitive non-targeted LC-MS/MS method. *PLoS One* 11:e0163469. doi: 10.1371/journal.pone.0163469
- Pearson, J. P., Pesci, E. C., and Iglesias, B. H. (1997). Roles of *Pseudomonas aeruginosa* las and rhl quorum-sensing systems in control of elastase and rhamnolipid biosynthesis genes. *J. Bacteriol.* 179, 5756–5767. doi: 10.1128/jb.179.18.5756-5767.1997
- Peter, J. A. C., Tiago, A., and Jeffrey, T. C. (2009). Biopython: freely available Python tools for computational molecular biology and bioinformatics. *Bioinformatics* 25, 1422–1423. doi: 10.1093/bioinformatics/btp163
- Pletzer, D., Lafon, C., Braun, Y., Köhler, T., Page, M. G. P., Mourez, M., et al. (2014). High-throughput screening of dipeptide utilization mediated by the ABC transporter DppBCDF and its substrate-binding proteins DppA1-A5 in *Pseudomonas aeruginosa*. *PLoS One* 9:e111311. doi: 10.1371/journal.pone.0111311
- Poonsuk, K., Tribuddharat, C., and Chuanchuen, R. (2014). Simultaneous overexpression of multidrug efflux pumps in *Pseudomonas aeruginosa* non-cystic fibrosis clinical isolates. *Can. J. Microbiol.* 60, 437–443. doi: 10.1139/cjm-2014-0239
- Poplin, R., Ruano-Rubio, V., DePristo, M. A., Fennell, T. J., Carneiro, M. O., Van Der Auwera, G. A., et al. (2017). Scaling accurate genetic variant discovery to tens of thousands of samples. *bioRxiv* [Preprint]. bioRxiv, 201178 doi: 10.1101/201178v2
- Preston, M. J., Fleiszig, S. M., Zaidi, T. S., Goldberg, J. B., Shortridge, V. D., Vasil, M. L., et al. (1995). Rapid and sensitive method for evaluating *Pseudomonas aeruginosa* virulence factors during corneal infections in mice. *Infect. Immun.* 63, 3497–3501. doi: 10.1128/IAI.63.9.3497-3501.1995
- Quale, J., Bratu, S., Gupta, J., and Landman, D. (2006). Interplay of efflux system, ampC, and oprD expression in carbapenem resistance of *Pseudomonas aeruginosa* clinical isolates. *Antimicrob. Agents Chemother.* 50, 1633–1641. doi: 10.1128/AAC.50.5.1633-1641.2006
- Rausch, T., Zichner, T., Schlattl, A., Stutz, A. M., Benes, V., and Korbel, J. O. (2012). DELLY: structural variant discovery by integrated paired-end and split-read analysis. *Bioinformatics* 28, i333–i339. doi: 10.1093/bioinformatics/bts378
- Ravel, J., and Cornelis, P. (2003). Genomics of pyoverdine-mediated iron uptake in pseudomonads. *Trends Microbiol.* 11, 195–200.
- Rice, P., Longden, I., and Bleasby, A. (2000). EMBOSS: the European molecular biology open software suite. *Trends Genet.* 16, 276–277. doi: 10.1016/S0168-9525(00)02024-2
- Robinson, J. T., Thorvaldsdóttir, H., Winckler, W., Guttman, M., Lander, E. S., Getz, G., et al. (2011). Integrative genome viewer. *Nat. Biotechnol.* 29, 24–26. doi: 10.1038/nbt.1754. Integrative
- Rust, L., Pesci, E. C., and Iglesias, B. H. (1996). Analysis of the *Pseudomonas aeruginosa* elastase (lasB) regulatory region. *J. Bacteriol.* 178, 1134–1140. doi: 10.1128/jb.178.4.1134-1140.1996
- Schuster, M., and Greenberg, E. P. (2006). A network of networks: quorum-sensing gene regulation in *Pseudomonas aeruginosa*. *Int. J. Med. Microbiol.* 296, 73–81. doi: 10.1016/j.ijmm.2006.01.036
- Sobel, M. L., Neshat, S., and Poole, K. (2005). Mutations in PA2491 (mexS) promote MexT-dependent mexEF-oprN expression and multidrug resistance in a clinical strain of *Pseudomonas aeruginosa*. *J. Bacteriol.* 187, 1246–1253. doi: 10.1128/JB.187.4.1246-1253.2005
- Stintzi, A., Evans, K., Meyer, J., and Poole, K. (1998). Quorum-sensing and siderophore biosynthesis in *Pseudomonas aeruginosa*: lasR/lasI mutants exhibit reduced pyoverdine biosynthesis. *FEMS Microbiol. Lett.* 166, 341–345. doi: 10.1111/j.1574-6968.1998.tb13910.x
- Stover, C. K., Pham, X. Q., Erwin, A. L., Mizoguchi, S. D., Warrener, P., Hickey, M. J., et al. (2000). Complete genome sequence of *Pseudomonas aeruginosa* PAO1, an opportunistic pathogen. *Nature* 406, 959–964. doi: 10.1038/35023079
- Suyama, M., Torrents, D., and Bork, P. (2006). PAL2NAL: robust conversion of protein sequence alignments into the corresponding codon alignments. *Nucleic Acids Res.* 34, W609–W612. doi: 10.1093/nar/gkl315
- Taguchi, F., and Ichinose, Y. (2011). Role of type IV pili in virulence of *Pseudomonas syringae* pv. tabaci 6605: correlation of motility, multidrug resistance, and HR-inducing activity on a nonhost plant. *Mol. Plant Microbe Interact.* 24, 1001–1011. doi: 10.1094/MPMI-02-11-0026
- Tanizawa, Y., Fujisawa, T., and Nakamura, Y. (2018). DFAST: a flexible prokaryotic genome annotation pipeline for faster genome publication. *Bioinformatics* 34, 1037–1039. doi: 10.1093/bioinformatics/btx713
- Tian, Z.-X., Fargier, E., Mac Aogain, M., Adams, C., Wang, Y.-P., and O'Gara, F. (2009a). Transcriptome profiling defines a novel regulon modulated by the LysR-type transcriptional regulator MexT in *Pseudomonas aeruginosa*. *Nucleic Acids Res.* 37, 7546–7559. doi: 10.1093/nar/gkp828
- Tian, Z.-X., Mac Aogain, M., O'Connor, H. F., Fargier, E., Mooij, M. J., Adams, C., et al. (2009b). MexT modulates virulence determinants in *Pseudomonas aeruginosa* independent of the MexEF-OprN efflux pump. *Microb. Pathog.* 47, 237–241. doi: 10.1016/j.micpath.2009.08.003
- Van der Auwera, G. A., Carneiro, M. O., Hartl, C., Poplin, R., del Angel, G., Levy-Moonshine, A., et al. (2013). From fastQ data to high-confidence variant calls: the genome analysis toolkit best practices pipeline. *Curr. Protoc. Bioinformatics* 43, 11.10.1–11.10.33. doi: 10.1002/0471250953.bi1110s43
- Walsh, F., and Amyes, S. G. B. (2007). Carbapenem resistance in clinical isolates of *Pseudomonas aeruginosa*. *J. Chemother.* 19, 376–381. doi: 10.1179/joc.2007.19.4.376
- Wick, R. R., Judd, L. M., Gorrie, C. L., and Holt, K. E. (2017). Unicycler: resolving bacterial genome assemblies from short and long sequencing reads. *PLoS Comput. Biol.* 13:e1005595. doi: 10.1371/journal.pcbi.1005595
- Wilder, C. N., Diggle, S. P., and Schuster, M. (2011). Cooperation and cheating in *Pseudomonas aeruginosa*: the roles of the las, rhl and pqs quorum-sensing systems. *ISME J.* 5, 1332–1343. doi: 10.1038/ismej.2011.13
- Winsor, G. L., Griffiths, E. J., Lo, R., Dhillon, B. K., Shay, J. A., and Brinkman, F. S. L. (2016). Enhanced annotations and features for comparing thousands of *Pseudomonas* genomes in the *Pseudomonas* genome database. *Nucleic Acids Res.* 44, D646–D653. doi: 10.1093/nar/gkv1227
- Winstanley, C., O'Brien, S., and Brockhurst, M. A. (2016). *Pseudomonas aeruginosa* evolutionary adaptation and diversification in cystic fibrosis chronic lung infections. *Trends Microbiol.* 24, 327–337. doi: 10.1016/j.tim.2016.01.008
- Ye, K., Schulz, M. H., Long, Q., Apweiler, R., and Ning, Z. (2009). Pindel: a pattern growth approach to detect break points of large deletions and medium sized insertions from paired-end short reads. *Bioinformatics* 25, 2865–2871. doi: 10.1093/bioinformatics/btp394
- Zhang, J., Wang, J., and Wu, Y. (2012). An improved approach for accurate and efficient calling of structural variations with low-coverage sequence data. *BMC Bioinformatics* 13(Suppl. 6):S6. doi: 10.1186/1471-2105-13-s6-s6
- Conflict of Interest:** The authors declare that the research was conducted in the absence of any commercial or financial relationships that could be construed as a potential conflict of interest.
- Publisher's Note:** All claims expressed in this article are solely those of the authors and do not necessarily represent those of their affiliated organizations, or those of the publisher, the editors and the reviewers. Any product that may be evaluated in this article, or claim that may be made by its manufacturer, is not guaranteed or endorsed by the publisher.
- Copyright © 2022 Liu, Ahator, Wang, Feng, Xu, Li, Zhou and Zhang. This is an open-access article distributed under the terms of the Creative Commons Attribution License (CC BY). The use, distribution or reproduction in other forums is permitted, provided the original author(s) and the copyright owner(s) are credited and that the original publication in this journal is cited, in accordance with accepted academic practice. No use, distribution or reproduction is permitted which does not comply with these terms.